Cellulose (2017) 24:3969–3980
DOI 10.1007/s10570-017-1405-8

ORIGINAL PAPER

Barrier and mechanical properties of plasticized and cross-linked nanocellulose coatings for paper packaging applications

Martha A. Herrera · Aji P. Mathew · Kristiina Oksman

Received: 23 March 2017 / Accepted: 8 July 2017 / Published online: 11 July 2017

ABSTRACT Barrier, mechanical and thermal properties of porous paper substrates dip-coated with nanocellulose (NC) were studied. Sorbitol plasticizer was used to improve the toughness, and citric acid cross-linker to improve the moisture stability of the coatings. In general, the addition of sorbitol increased the barrier properties, maximum strength and toughness as well as the thermal stability of the samples when compared to the non-modified NC coatings. The barrier properties significantly improved, especially for plasticized NC coating's, where the oxygen permeability value was as low as 0.7 mL μm day^{-1} m^{-2} kPa^{-1} at 49% RH and the water vapor permeability was reduced by 60%. Furthermore, we found that the cross-linked plasticized NC coating had a smoother surface (50% lower roughness) compared to non-modified ones. This study shows that the environmentally friendly additives sorbitol and citric acid had positive effects on NC coating properties, increasing its potential use in paper-based packaging applications.

Keywords Nanocellulose · Dip-coating · Plasticizing · Cross-linking · Barrier properties

M. A. Herrera · A. P. Mathew · K. Oksman
Division of Materials Science, Luleå University of Technology, SE-97187 Luleå, Sweden
e-mail: herrerarodriguez@gmail.com

A. P. Mathew
e-mail: aji.mathew@mmk.su.se

A. P. Mathew
Department of Materials and Environmental Chemistry, Stockholm University, SE-106 91 Stockholm, Sweden

K. Oksman (✉)
Fiber and Particle Engineering, University of Oulu, Oulu, Finland
e-mail: kristiina.oksman@ltu.se

Introduction

Porous cellulose-based materials, such as paperboard, have a great impact in the packaging industry due to their eco-friendly nature and biodegradability. However, hydrophilic behavior and a porous structure prevent the use of paper in a wide range of applications. To overcome this issue, paper is usually coated in combination with other materials, such as plastic or aluminum, that provide improvements in barrier properties at the expense of its eco-friendly and biodegradable nature. A more ecological way to solve the problems linked to porous cellulose-based materials is the coating with bio-based resources, such as nanocellulose (NC) (Herrera et al. 2016). Although NC particles have been used to coat porous cellulose-based materials, their ability to form rigid three-dimensional networks, can represent a problem that restricts their use in applications where flexibility is needed (Syverud and Stenius 2009; Aulin et al. 2010; Herrera et al. 2014; Lavoine et al. 2014; Herrera et al. 2016).

One way to increase the flexibility of the NC coating is to reduce the amount of hydrogen bonds using

plasticizers, such as sorbitol (Mathew et al. 2008) or glycerol (Xiao et al. 2003; Hansen et al. 2012; Liu et al. 2013; Wang et al. 2015). These plasticizers have been shown to increase the tensile strength (Xiao et al. 2003; Liu et al. 2013; Mathew et al. 2008; Wang et al. 2015) and the oxygen barrier (Hansen et al. 2012) of films.

Another method to improve the dimensional stability and increase the hydrophobicity of coatings is through chemical cross-linking (esterification). The cross-linking procedure consists on the functional modification of the NC without its disintegration (de Cuadro et al. 2015). Different chemicals, such as toluenesulfonic acid, hexanoic acid (Matsumura et al. 2000), butyryl, benzoyl, naphtoyl, diphenyl acetatyl, and stearoyl (Vuoti et al. 2013) have been used to carry out this chemical cross-linking. However, poly(carboxylic acid)s, such as citric acid (de Cuadro et al. 2015; Quellmalz and Mihranyan 2015) or succinic acid (Zhou et al.1995), have become very popular because of their environmentally friendly and non-toxic nature. The cross-linking technique has also been used to improve the wet strength of cellulosic materials (Zhou et al. 1995; Quellmalz and Mihranyan 2015) and to decrease the solubility in water of polysaccharides (Sirviö et al. 2014).

The main goal of this study was to investigate the effect of the plasticizer sorbitol and the cross-linker citric acid (CA) on NC coatings. The end groups of sorbitol are hydroxyl terminated (OH) and are therefore expected to cross-link with CA in the same way as the cellulose hydroxyl groups (see Fig. 1). Although plasticizers and cross-linking processes have been used before, to the best of the author's knowledge, this is the first time that nanocellulose coatings plasticized with sorbitol and, at the same time, cross-linked with CA, are studied. The purpose was to study the effect of the plasticization and cross-linking on the barrier and mechanical properties as well as the thermal stability of prepared coatings.

Experimental

Materials

A suspension of nanocellulose (NC), with a dry weight of 1.5 wt% was obtained from purified cellulose from a bioethanol processing route (SEKAB, Örnsköldsvik, Sweden). The process is described elsewhere by Mathew et al. (2014), and the raw material characteristics of this

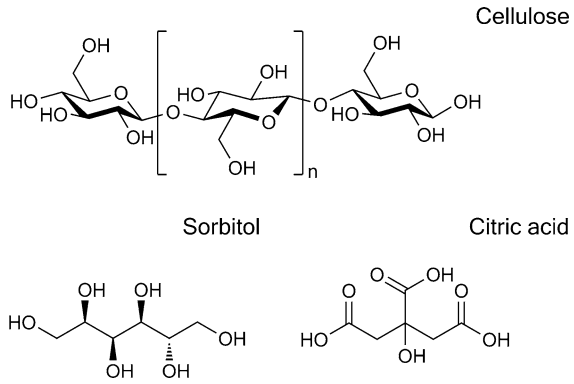

Fig. 1 Chemical structures of cellulose, sorbitol and citric acid (CA)

specific nanocellulose are described more in detail elsewhere (Herrera et al. 2014; Mathew et al. 2014; Moberg et al. 2017). Briefly, a bioethanol residue containing lignin and cellulose was purified, the remaining highly crystalline cellulose (concentration of 1.5 wt%) was isolated to nanosize using a high-pressure homogenizer APV 2000 (Denmark) with a pressure of 500 bars until a thick gel was formed. The crystallinity of this nanocellulose was reported to be about 77% measured with XRD and have carboxyl and aldehyde functional groups (Mathew et al. 2014). The dimensions were approx. 520 nm in length and 5.6 nm in diameter reported by Moberg at el. (2017). This is an interesting nanocellulose as the length is longer that usual cellulose nanocrystals hydrolyzed from wood sources (200 nm) and have a different surface chemistry.

D-sorbitol (98%) Alfa Aesar (Darmstadt, Germany) was used as the plasticizer, citric acid anhydrous (CA) from Merk (Hohenbrunn, Germany) was used as the cross-linking agent, and sodium hypophosphite monohydrate as the catalyst for the cross-linking reaction, from Alfa Aesar (Steinheim, Germany), were purchased from Sigma Aldrich and used as received without further modification. Whatman cellulose filter paper no 1, with a pore size of 11 μm, was used as a substrate. The substrate was cleaned before coating by rinsing three times with the constant addition of acetone and deionized water.

Preparation of the coatings

Layer-by-layer coatings were performed on the porous substrate, immediately after cleaning, using the dip-coating (D-C) technique. The substrate was immersed

in NC suspension (1.5 wt%) for 2 min. After this, the sample was completely immersed in a rinse bath of deionized water for 10 s. The substrate was then left to dry at ambient conditions for 24 h before the dipping was repeated. This procedure defines one layer, and it was repeated until coatings with 3 and 6 layers were prepared. This procedure was repeated with sorbitol added to the NC suspension at a ratio of 1:4 sorbitol to NC. After these steps, cross-linking was performed on all these samples. The coatings were cross-linked by submerging the coated substrates in a water solution containing 20 wt% citric acid (CA) and 3 wt% sodium hypophosphite monohydrate. The samples were kept in this solution for 2 h, and the cross-linking was performed at room temperature and left to dry at 21 °C for 6 h. After that, the coatings were dried in an oven at 80 °C overnight and cured at 150 °C for 5 min and left at ambient conditions for 20 min. After this, the samples were immersed in a rinse bath of deionized water until the pH of the water was neutral. Next, the samples were left to dry at ambient conditions for 2 h and then were kept at 80 °C for another 2 h. With this procedure, the cross-linked samples were obtained. Finally, four different types of coatings were prepared, including pure NC coatings, plasticized NC coatings (NC-S), cross-linked NC coatings (XNC), and plasticized and cross-linked NC coatings (XNC-S). As control samples, substrates were immersed in deionized water following the same procedure, but using only water. The sample coding and the materials described are given in Table 1. All the samples were kept in a desiccator at room temperature and 13% humidity.

Characterization of the coatings

The functional groups present in the coatings prepared before and after cross-linking with CA were characterized using Fourier Transformation Infrared spectroscopy (FT-IR) with a Varian 670-IR spectrometer (Specac, UK). Dried films of the coated samples were used to record the attenuated total reflectance Fourier transform infrared (ATR-FTIR) spectra. The spectra were recorded at room temperature in the range from 4000 to 390 cm^{-1} with 4 cm^{-1} resolution and an accumulation of 32 scans.

A scanning electron microscope (SEM), JEOL JSM-6460LV (Tokyo, Japan), was used to measure the thickness of the samples from fractured surfaces. The cross sections of the samples were coated with gold and studied at different magnifications. The thickness values are an average of approximately 20 measurements of 5 different images with different magnifications. The detailed coating network was observed, and the surface roughness (Ra) was measured from the images of the coatings obtained from the atomic force microscopy (AFM) Nanoscope V, Veeco Instruments (Santa Barbara, CA, USA), using tapping mode at 20 °C and 23% RH. The antimony-doped silica cantilever was oscillated at its fundamental resonance frequency ranging between 320 and 364 kHz, and no image processing except flattening was used. The Ra is the average of the measurements performed on 5 different images on a surface area of 1 μm^2.

Samples with dimensions of 10 mm × 10 mm × specific thickness were dried for 18 h at 100 °C. The grammage of the coating was calculated as the difference between the coated sample weight (in grams) minus the uncoated sample weight (in grams) divided by the total area (in m^2), as shown in Eq. 1:

$$CG = (W_{coated} - W_{uncoated})/Area \quad (1)$$

Thermogravimetric analysis (TGA) using a TA instrument TGA Q500 (New Castle, USA) of the samples was carried out to investigate their thermal stability The temperature range was set from 30 to 600 °C in a nitrogen atmosphere with a ramp mode and a heating rate of 5 °C/min.

The mechanical properties of the samples were measured at ambient conditions (21 °C and 35% RH) using a Shimadzu AG–X universal tensile testing machine (Japan). The samples were conditioned at 60% RH for three days before testing. A load cell of 1 kN was used, the gauge length was 20 mm, and the crosshead speed of 2 mm/min was used on samples 5 mm wide, 20 mm long and of the specific thickness for each sample (see Table 2). The elongation at break and tensile strength were directly obtained from the data, but the toughness and tensile modulus were calculated from the stress–strain curves. The values reported are the average of four samples.

The moisture uptake of the uncoated substrates as well as all produced coatings was determined to obtain the changes in the moisture uptake behavior when changing the coatings. This procedure is a modification of the one used by Mathew and Dufresne (2002). Samples with dimensions 10 mm × 10 mm × thickness were cut and dried at 100 °C for 18 h. After this,

Table 1 Prepared material combinations

Sample coding	Description of the materials
Control	Pure substrate treated 6 times with water
NC3	NC coated substrate, 3 layers
NC3-S	Plasticized NC-Sorbitol coated substrate, 3 layers
X-NC3	Cross-linked NC coated substrate, 3 layers
X-NC3-S	Cross-linked and plasticized NC-Sorbitol coated substrate, 3 layers
NC6	NC coated substrate, 6 layers
NC6-S	Plasticized NC-Sorbitol coated substrate, 6 layers
X-NC6	Cross-linked NC coated substrate 6 layers
X-NC6-S	Cross-linked and plasticized NC-Sorbitol coated substrate, 6 layers

Table 2 Thickness, grammage and roughness of the NC coatings with sorbitol and citric acid

Materials	Thickness (μm)	Roughness (nm)	Grammage (g/m^2)	BET pore size (Å)	BET surface area (m^2/g)
Control	–	19 ± 6	–	82.9	5.27
NC3	10 ± 2	5 ± 1	42 ± 2	63.3	2.98
NC3-S	6 ± 1	8 ± 2	35 ± 2	*	*
X-NC3	30 ± 1	5 ± 1	61 ± 2	68.2	2.03
X-NC3-S	25 ± 4	5 ± 1	79 ± 8	*	*
NC6	26 ± 6	4 ± 1	70 ± 3	61.1	2.65
NC6-S	16 ± 5	5 ± 1	54 ± 2	61.0	0.34
X-NC6	50 ± 5	7 ± 1	95 ± 3	65.1	1.78
X-NC6-S	54 ± 6	6 ± 1	130 ± 2	15.3	15.9

* Not studied

the samples were weighed (M_o) and placed in a desiccator at 95% RH and room temperature. The samples were removed at different time intervals (t) and weighed (M_t) until the equilibrium weight (M_∞) was reached. The moisture uptake was calculated following Eq. 2. The values reported are the average of three samples for each type of coating.

$$MU = (M_t - M_o)100\%/M_o \quad (2)$$

The water vapor transmission rate (WVTR) and water vapor permeability (WVP) of the uncoated and coated samples were determined using a modification of the standard ASTM E 96. The samples were glued using hot silicon on the top of a glass flask (diam. 23 mm) filled with 20 mL distilled water. The container was weighed and placed in a desiccator at an average temperature and humidity of 22 °C and 60% RH, respectively, and weighed at regular time intervals over five weeks. Duplicates were tested for all materials. The WVTR was calculated according to Eq. 3:

$$WVTR = (\Delta m/\Delta t)/A \quad (3)$$

where m is the mass variation (in grams), Δt is the time variation (in days), and A is the exposed area of the sample (in m^2). The WVP was calculated according to Eq. 4:

$$WVP = WVTR \times L/\Delta P \quad (4)$$

where L is the thickness of the sample (in meters) and ΔP is the difference in vapor pressure of the two sides of the films (in kPa).

The oxygen permeability (OP) of the uncoated and coated samples was measured using Agilent Technologies ADM2000 universal gas flow meter 2850 (Wilmington, USA) at 22 °C and 49% RH. A constant gas flow at a pressure of 0.2 bar (15 cm Hg) was applied to the samples, and the exit flow was registered to calculate the oxygen permeability (OP) using the variable pressure model (Joly et al. 1999; Belbekhouche et al. 2011) and unit convertor. The values reported are the average of four samples for each type of coating.

Results and discussions

Cross-linking

Cross-linking of cellulose with CA is believed to occur due to the dehydration, through an esterification process producing an ester group that can link with the available hydroxyl group on the cellulose, as seen in Fig. 2.

The cross-linking efficiency is estimated using the molecular weight (MW) of the cellulose monomer (182 g/mol) and the grammage of the prepared coating (42 g/m^2 NC3). This results in 0.35 mol/m^2 glucose units per m^2 of the coating. After the cross-linking, the grammage of the NC3 coating increased from 42 to 61 g/m^2, indicating that the addition of the CA was 19 g/m^2 (as seen in Table 2). Knowing that the MW of the CA is 207 g/mol, it is then calculated that the amount of CA per m^2 of coating is 0.1 mol/m^2. If each molecule of CA connects with 2 units of glucose (as shown in Fig. 2), then 0.2 mol of glucose are cross-linked in the X-NC3. This implies that 87% of the glucose units can be involved in the crosslinking. When the same calculation is performed for X-NC6, it can be found that 69% of the glucose units can take part in the crosslinking. These theoretical estimations indicated that more than half of the glucose units are cross-linked. (*note that the effect of crystallinity of CNC on crosslinking is not considered in the calculations)*. This high degree of cross-linking is however not realistic, given that a large amounts of the cellulose molecules are inside the CNC crystals and thus not available for crosslinking. The high degree of crosslinking based on calculations also can be due to an overestimation of the grammage of CA. The results in Table 2 shows a significant increase in grammage after crosslinking in the case of plasticized and unplasctisized coatings with different CNC concentrations. De Cuadro et al. (2015) have also shown a similar increase of the weight when filter paper was cross-linked with CA; they suggested that the reason was the accumulation of the acid attached to the cellulose after the esterification process.

The FT-IR study was conducted to prove the esterification process, after the cross-linking with CA, through the verification of the introduction of the ester groups. In Fig. 3 (a and b) for the samples without CA treatment (NC6 and NC6-S), some characteristic peaks can be identified. The peak at approximately 3300 cm^{-1} corresponds to O–H groups, at 2900 cm^{-1}, the peak corresponds to C–H groups, and at approximately 1000 cm^{-1}, the peak corresponds to C–O groups. These peaks correspond to the cellulose structure (Joly et al. 1999; Thanh and Nhung 2009; De Cuadro et al. 2015). When analyzing the FT-IR of the samples after crosslinking with citric acid (X-NC6 and X-NC6-S), a new and strong absorption band appears at approximately 1720 cm^{-1} that corresponds to the C=O group from the esters introduced after the esterification process. These ester groups are the ones that link with the hydroxyl groups of the cellulose after the esterification process and introduce the crosslinking between cellulose chains.

Microstructure and roughness

The surface roughness of the samples was measured using AFM images, as in Fig. 4, and the Ra values are shown in Table 2. The roughness of the coated samples was always lower than the one measured for the control sample (uncoated), showing that the coating reduced the surface roughness from 19 to 4–8 nm. The roughness of the coated samples was also very similar. There were no significant differences

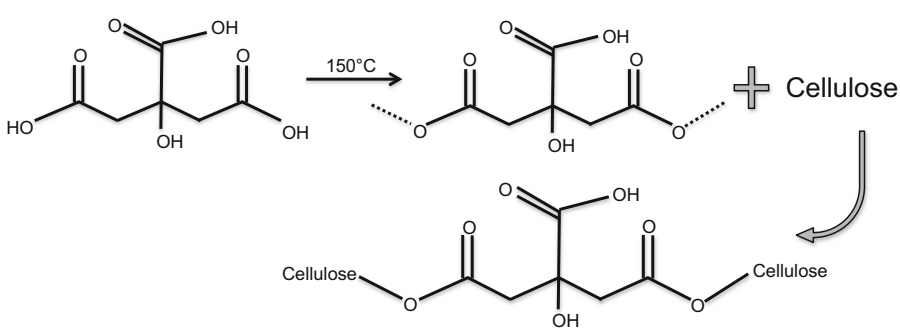

Fig. 2 Proposed mechanism for the cross-linking of cellulose with citric acid

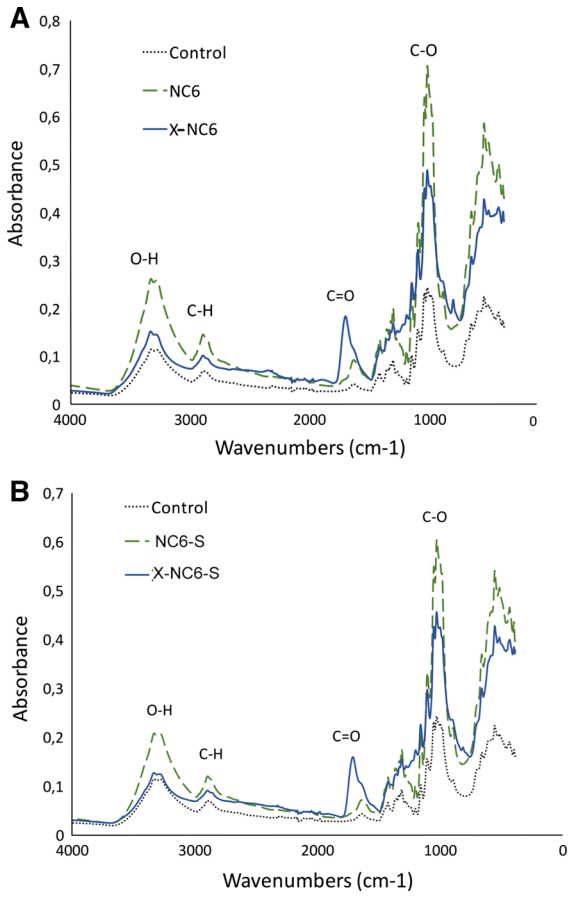

Fig. 3 FT-IR spectra of **a** NC6 (*Control*) and cross-linked X-NC6 coatings and **b** plasticized NC6-S and crosslinked X-NC6-S coatings with the control sample in each case, confirming the crosslinking

between the pure NC, NC-S, or their cross-linked versions (X-NC and X-NC-S). This indicates that the surface roughness is not affected by the addition of sorbitol or by the cross-linking with CA. Additionally; Fig. 4 shows that the NC has formed a dense and uniform network. Cellulose has a strong tendency towards self-association, making the formation of film-like structures easy. This dense arrangement of NC was previously reported in several studies (Li et al. 2013; Herrera et al. 2014, 2016).

Cross-section SEM images of the porous control sample as well as the thin and dense NC3-S coating on the substrate surface can be seen in Fig. 5. From the figures, it is clear that the dip coating resulted in coated substrate and that the NC was not impregnated into the substrate. The SEM images show that the NC coatings displayed a layered structure typical for the nanocellulose coatings (Aulin et al. 2010; Herrera et al. 2016). The thickness of the coatings was measured from the cross sections and used to calculate the grammage; the values are presented in Table 2. As expected, the thickness and grammage of the six-layer coatings were twice that of the three layer coatings in all cases. Table 2 shows that the plasticizer decreased both the thickness and grammage of the coatings, which is probably related to the differences in the densities of sorbitol (1.489 g/cm^3) and cellulose (1.599 g/cm^3) (Sugiyama et al. 1991). When the cross-linking was complete, the thickness and grammage of the coatings were increased when compared with their non-cross-linked counterparts. The weight gain observed after the cross-linking is due to the accumulation of the CA attached by esterification into the hydroxyl groups in the nanocellulose fibers (De Cuadro et al. 2015) and sorbitol (Sugiyama et al. 1991). This weight and thickness gain indicates a successful crosslinking, as shown in an earlier study (De Cuadro et al. 2015).

BET analysis was carried out to understand the effect of the number of coated layers, plasticizer addition and cross-linker addition on the pore size and surface area of the barrier layers; the values can be found in Table 2. The pore size is in the nanometer range and decreased in all cases compared to the control after the coating with NC which is expected. The cross-linking did not significantly affect the pore size of the coatings. However, a dramatic reduction in the pore size was observed in the cross-linked plasticized samples (X-NC6-S). In a similar way, the surface area of NC and X-NC samples are alike, but the surface area of the corresponding plasticized samples increased by sixfold. BET studies showed that a combination of plasticizer and cross-linker decreased the pore size and increased the surface area of the barrier layer.

Thermal stability

The thermogravimetric analysis of the coatings produced in this study was carried out to evaluate how the plasticizer and cross-linking process affected the thermal stability of the samples, and as a confirmation of the cross-linking. The onset temperature, maximum degradation temperature and residue at 600 °C are shown in Table 3.

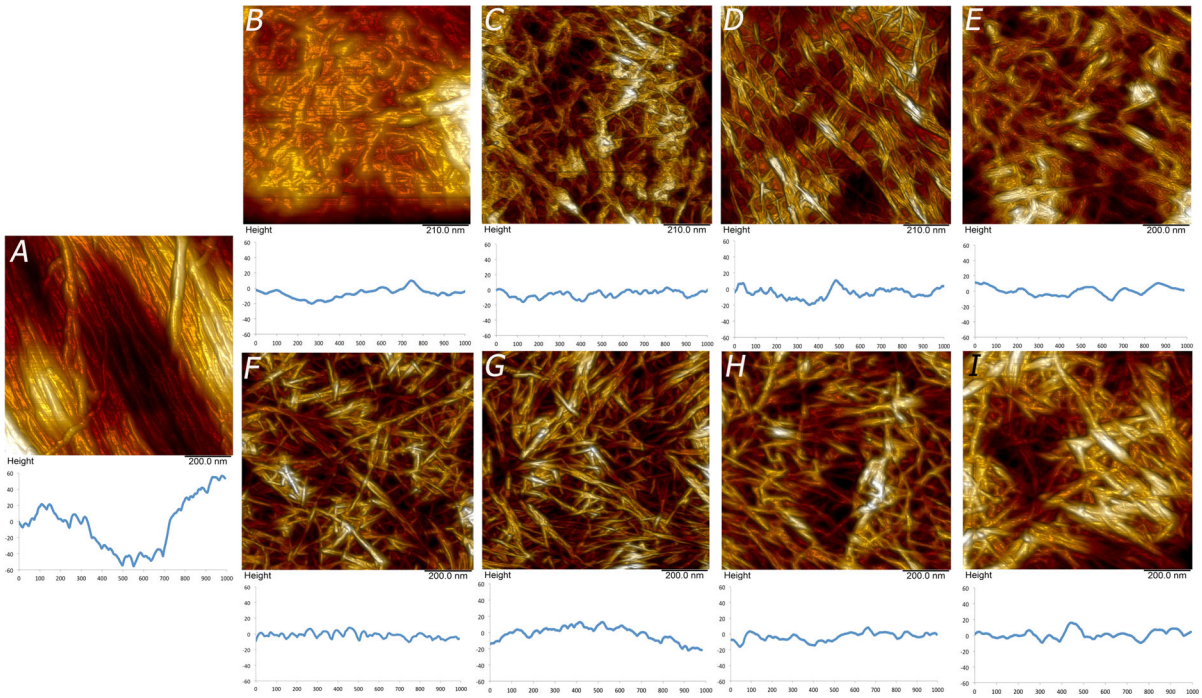

Fig. 4 AFM height images of **a** the uncoated substrate, **b** NC3, **c** NC6, **d** NC3-S, **e** NC6-S, **f** X-NC3, **g** X-NC6, **h** X-NC3-S, and **i** X-NC6-S. The scanned surface area is 1 m^2 in all materials. The typical height profiles are shown below each image, all with a Z-range of 60 nm and a X-range of 1000 nm, showing the roughness profile of the coatings

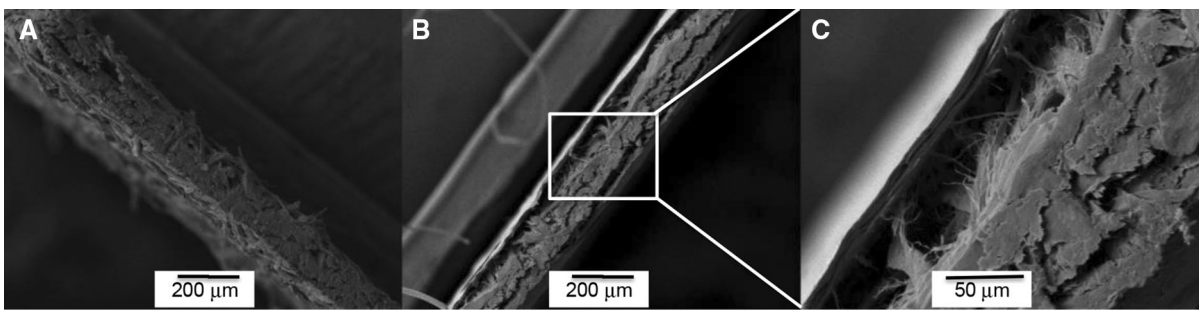

Fig. 5 Comparison of the cross-sections of the pure substrate and the NC3-S coating. **a** Control, **b** NC3-S and **c** NC3-S at higher magnification showing the dense coating layer and porous substrate

In general, the plasticization and the cross-linking of the NC did not affect the thermal properties of the coatings; their onset temperatures are approximately 300 °C. However, the plasticized and cross-linked coatings showed slightly lower onset temperatures. This indicates that the combination of sorbitol and citric acid slightly lowers the thermal stability of the coatings. The maximum degradation temperature increased with the addition of the sorbitol (20 wt %) to the coating, increasing the thermal stability of the whole system. Mathew et al. (2008) reported similar improvements of the thermal stability of tunicin nanocomposites when sorbitol was used as a plasticizer (Mathew et al. 2008). Moreover, the increase in the thermal stability in samples containing nanofibrillated cellulose and sorbitol was described by Hansen et al. (2012). They reported that the use of sorbitol plasticizer resulted in a higher thermal stability than other plasticizers, such as glycerol (Hansen et al. 2012). Table 3 also shows that the residue at 600 °C

Table 3 The thermal stability of the NC films, the onset temperature, maximum degradation temperature, and residue at 600 °C, obtained by the TGA

Materials coating	Onset temp. (°C)	Max. degrad. temp. (°C)	Residue at 600 °C (%)
Control	311 ± 1	325 ± 0	9 ± 0
NC3	287 ± 0	324 ± 2	20 ± 1
NC3-S	309 ± 8	350 ± 8	19 ± 8
X-NC3	293 ± 7	332 ± 8	19 ± 1
X-NC3-S	288 ± 12	328 ± 1	36 ± 2
NC6	298 ± 4	340 ± 0	15 ± 0
NC6-S	302 ± 7	351 ± 11	15 ± 2
X-NC6	298 ± 3	330 ± 1	22 ± 3
X-NC6-S	270 ± 5	324 ± 1	30 ± 0

Table 4 Tensile strength, strain at failure, Young's modulus and toughness of the samples

Materials	Max strength (MPa)	Max.strain (%)	Young's modulus (MPa)	Toughness (MJ/m^3)
Control	7.8 ± 0.4	2.5 ± 0.1	570 ± 30	3.9 ± 0.2
NC3	8.9 ± 1.8	2.0 ± 0.3	580 ± 70	3.6 ± 0.5
NC3-S	12.2 ± 0.7	2.7 ± 0.3	540 ± 70	6.2 ± 0.4
X-NC3	6.1 ± 1.1	4.0 ± 0.6	280 ± 40	10.6 ± 0.4
X-NC3-S	7.7 ± 1.5	3.7 ± 0.4	310 ± 10	10.1 ± 0.5
NC6	10.6 ± 3.7	2.4 ± 0.1	500 ± 40	5.4 ± 0.4
NC6-S	10.3 ± 1.4	2.6 ± 0.3	490 ± 80	6.2 ± 0.3
X-NC6	5.8 ± 1.9	3.0 ± 0.8	280 ± 60	6.4 ± 0.5
X-NC6-S	5.7 ± 0.5	2.5 ± 0.4	330 ± 10	3.9 ± 0.3

increased when the coatings were cross-linked, which may be another indication of the successful cross-linking of the cellulose with the citric acid.

Mechanical properties

Table 4 shows the mechanical properties of the control and coated samples.

In general, the addition of the nanocellulose coating on the paperboard is expected to increase its mechanical properties. In this study, the addition of NC did not significantly improve the modulus, but the strength was slightly improved. The addition of the plasticizer had a positive effect on the strength as well as the toughness. When comparing the control sample with the plasticized coatings, in general, an increase of the maximum strength is observed, and it reaches a maximum value for the NC3-S coating (12.2 ± 0.6 MPa). The maximum strain remained similar between the control sample (2.5 ± 0.1%) and all the coated samples. The Young's modulus remained the same while the toughness increased among the non-cross-linked coatings, except for NC3, where the toughness remained similar. Thus, it is concluded that the plasticization improved the mechanical properties of the paper. The effect of sorbitol on the mechanical properties of the cellulose films was previously studied by Hansen et al. (2012) and Liu et al. (2013), and they reported a general increase in the maximum strength values when compared with the samples without sorbitol, as seen in the coatings of this study. The H-bonding (originating from electrostatic and charge transfer), and stacking interactions (originating from van der Waals interactions and hydrophobic forces) determine the biomolecular structure of the cellulose layer (Muller-Dethlefs and Hobza 2000). For this reason, the increase observed in the maximum strength and toughness is probably caused by a formation of new hydrogen bond networks and stacking interactions between the nanocellulose and the sorbitol (Liu et al. 2013).

When the coatings were cross-linked, a pronounced decrease in the maximum strength is observed, reaching the lowest value with X-NC6-S. The

maximum strain generally increased, except for X-NC6-S, where the value was the same as for the control sample. Additionally, the Young's modulus suffered a prominent decrease, almost half of the value achieved for the control sample, in all the cross-linked samples. And finally, for the cross-linked coatings, a general increase in the toughness was observed when compared with the control sample, with the exception of X-NC6-S which remained almost invariable. Thus, it is concluded that the cross-linking deteriorates the mechanical properties of the substrate in the conditions tested. The cross-linking process has been used to decrease the solubility of polysaccharides, such as cellulose, in water (Sirviö et al. 2014) and to increase the wet strength of paper through the creation of bridges between the cellulose fibers (Zhou et al. 1995; Quellmalz and Mihranyan 2015). When nanocellulose-coated papers were cross-linked with citric acid, a decrease in the maximum strength in dry condition was observed when compared with non-cross-linked papers. Additionally, it has been observed that cross-linking increases the pore volume and size of nanocellulose based paper filter, giving an indication of the reason why the mechanical properties did not improve as expected (Quellmalz and Mihranyan 2015). However, in wet conditions, the cross-linking confers improved tensile strength compared with non-cross-linked samples due to stability of the ester linkages introduced during the esterification reaction (Zhou et al. 1995).

Barrier properties

The moisture absorption of the control and the coated samples determined as a function of time is plotted in Fig. 6. All of the samples absorbed moisture, and this uptake was especially fast in the initial zone (<100 h). After this fast sorption zone, the moisture uptake rate decreased, leading to a plateau that corresponds to equilibrium swelling. The addition of NC coatings to the substrate decreased the equilibrium moisture uptake by almost half, passing from 29% for the control sample to 16% for NC6 (see Fig. 6). Although it has been shown that the coating of microfibrillated cellulose on porous substrates increases the moisture uptake when compared to the uncoated substrate (Lavoine et al. 2014), an opposite behavior was observed in this study, most probably due to the high crystallinity and nanometric nature of the cellulose

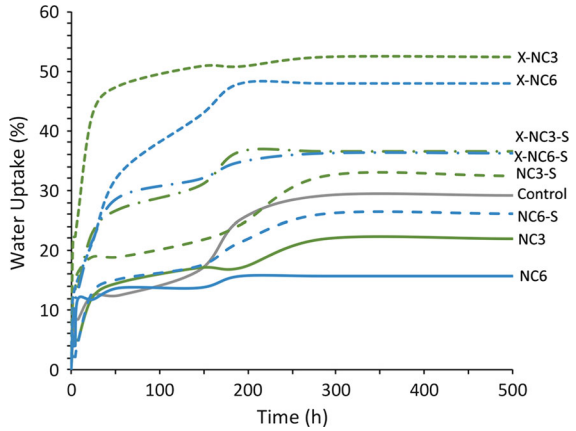

Fig. 6 Moisture uptake during conditioning at 95% RH versus time for the control and coated samples

used, as described in our earlier study (Herrera et al. 2016). Additionally, this moisture uptake decrease is expected to be because of the dense and uniform network formed by the NC (see Figs. 4 and 5), which helps to prevent the water from penetrating and reaching the more absorbable substrate. It was observed that the addition of sorbitol increased the equilibrium moisture uptake for the coatings, passing from 22 to 32% for NC3 and NC3-S, respectively, and from 16 to 26% for NC6 and NC6-S, respectively. The increase in the equilibrium moisture uptake when plasticizers are used has also been reported by others (Muller-Dethlefs and Hobza 2000; Mathew and Dufresne 2002). Additionally, a decrease in the moisture uptake with the increase in the layers of nanocellulose was observed. However, the addition of sorbitol and cross-linking of the samples produced an increase in the moisture uptake, reaching values of 52% for sample X-NC3.

The water vapor transmission rate (WVTR) and water vapor permeability (WVP) of the samples were measured and are graphically illustrated in Fig. 7. The WVTR values of the coated samples are lower for all coatings when compared with the control sample. An increase in the WVTR is observed with the addition of sorbitol on NC3 coatings but this increase is not as prominent for the NC6 coatings. Due to the great water-binding ability of sorbitol and its high swelling capability in the presence of water this material tends to have poor water vapor barrier properties (Yoo and Lee 1993; Pasupuleti and Madras 2011; Tammelin and Vartiainen 2014). For this reason, a pronounced increase in the WVTR in both cases (NC3-S and

NC6-S) was expected. The cross-linking decreased the WVTR for sample X-NC3 when compared with NC3. Samples X-NC6 and X-NC3-S continued with the same values as their non-cross-linked counterparts, while X-NC6-S increased when compared to NC6-S. Despite this, the WVTR values for all the coated samples are still lower than the value obtained for the control sample. When comparing the values obtained in this study with the WVTR of pure microfibrillated cellulose films (234 g m^{-2} day^{-1}) obtained by Rodionova et al. (2010), the most of the WVTR that were obtained were below this value. To take into account the differences in the thicknesses of the coatings, the WVP was studied, and the values are shown in Fig. 7. Generally, in all the cases, the WVP was reduced by more than half of the value of the control and the all the NC3 coatings showed to have lower WVP compared to the thicker NC6 coatings. When comparing these values, for example, with WVP of cellophane 0.6 g mm kPa^{-1} m^{-2} day^{-1} (Peroval et al. 2002), the coatings were in the same range.

In Fig. 8, the oxygen permeability of the control and coated samples measured at 49% RH are shown. The coatings produced a reduction of the OP when compared with the control sample, and the lowest value was obtained with the thinnest sample (NC3-S). The plasticization or the cross-linking decreased the OP of NC3 and NC6. However, the combination of plasticizer and crosslinking did not have a positive impact on the OP.

In general, the addition of plasticizer increased the oxygen barrier, whereas crosslinking decreased the barrier towards oxygen. It was also interesting to observe that the NC3 coatings displayed lower OP than the corresponding NC6 ones. The thinnest coating (6 μm) based on NC and sorbitol resulted in the best oxygen barrier. Further more, the addition of the sorbitol had also a positive effect on the thicker coating (NC6) while the cross linker is increasing the OP on both coatings.

The coatings produced in this study were either similar or better oxygen barriers when comparing their OP with values found in the literature for microfibrillated cellulose films (3.52–5.03 mL μm day^{-1} m^{-2} - kPa^{-1} at 50% RH) by Syverud and Stenius (2009), cellulose nanofibrils films (0.4 mL μm day^{-1} m^{-2} - kPa^{-1} at 50% RH) by Chinga-Carrasco and Syverud (2012), PET films (10–50 mL μm day^{-1} m^{-2} kPa^{-1} at 50% RH) or PS films (987–1481 mL μm day^{-1} - m^{-2} kPa^{-1} at 50% RH) by Lange et al. (2003). Usually, films made of hydrophilic polymers present high barriers against oxygen at low relative humidity (RH) because of the large amount of hydroxyl groups (OH) in their structure (see Fig. 1). This occurs due to the low polarity of oxygen, which produces a weak interaction with the highly polar hydroxyl groups of the polymer. When the relative humidity increases, the hydroxyl groups interact with the highly polar water molecules, weakening the hydrogen bonds that hold the polymer chains together. The loosening of these bonds releases the structure of the polymer, leading to increased OP at high RH (Tammelin and Vartiainen 2014). However, cellulose nanofibers have demonstrated a low OP even at high RH when compared with other natural polymers. The reason might be the fibrillar substructure of the cellulose, which has tightly packed crystalline regions that are impermeable to water. The crystalline regions increase the tortuous

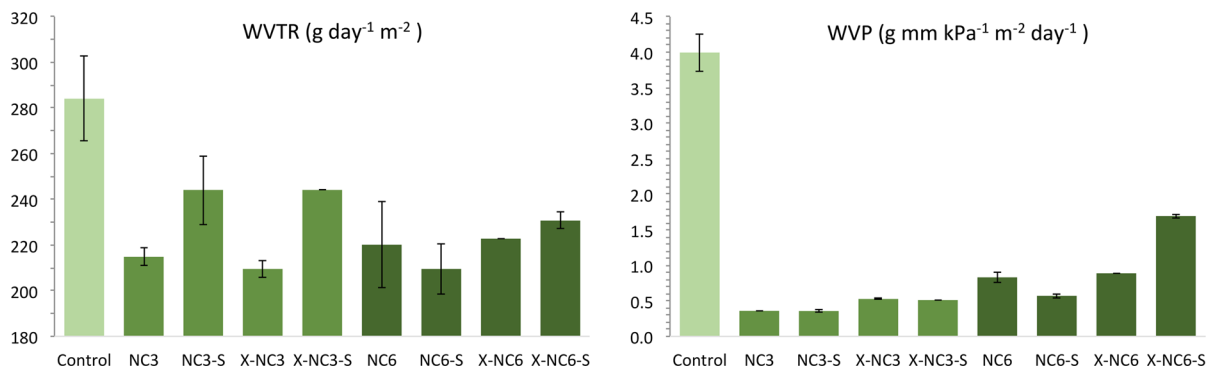

Fig. 7 WVTR and WVP of the prepared coatings compared to the control show that the nanocellulose coatings decreases the water vapor transmission rate and the water vapor permeability compared to the control material (average of two measurement showing that the values are on same range)

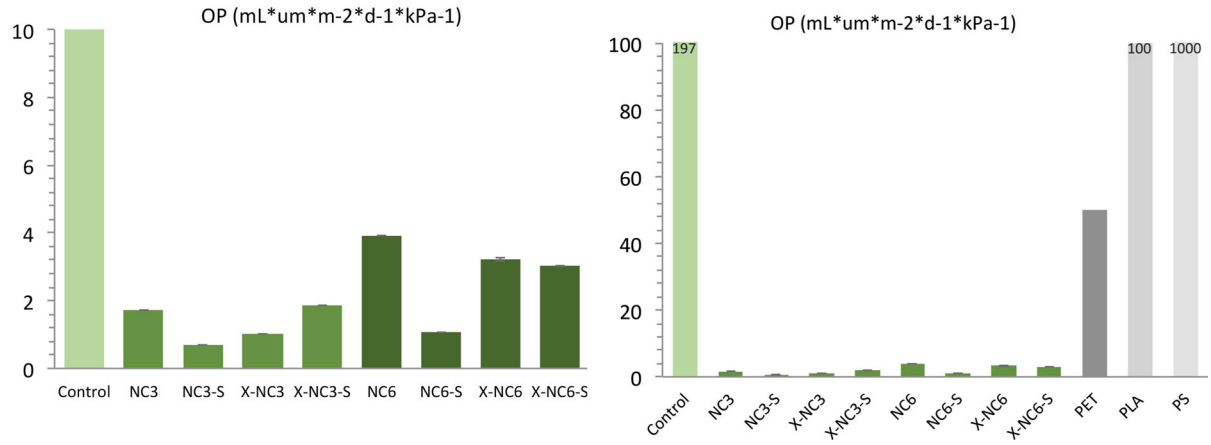

Fig. 8 OP for the control and coatings prepared. The prepared coatings are compared with common used plastic coatings PS, PET and also with PLA, a biopolymer (the error bars represent standard deviation)

diffusion path for molecules to permeate through the films (Herrera et al. 2014; Tammelin and Vartiainen 2014), along with a strong and dense film structure.

Conclusions

Porous paper substrates were successfully dip-coated with nanocellulose to two different coating thicknesses. Plasticization and cross-linking were used to improve the toughness and barrier properties towards water vapor and oxygen permeability. The crosslinking of cellulose with citric acid in the presence of sorbitol (plasticizer) was confirmed by FTIR analysis.

The thinner coating of plasticized NC (NC3-S), showed improved strength and toughness and lead to the lowest oxygen permeability 0.7 mL µm day^{-1} - m^{-2} kPa^{-1} at 49% RH and water vapor permeability 0.36 g mm kPa^{-1} m^{-2} day^{-1}. The moisture uptake was, in general, lower for the coatings compared to the control material, and the coated materials showed good thermal stability, being approximately 300°C. For all the NC coatings, irrespective of the number of layers, plasticizer and cross-linker content showed decreased water vapor permeability than the used porous paper substrates. Similarly, the oxygen permeability of all of the NC coated samples were better than the substrate as well as commonly used polymer barrier films, such as PET, PLA and PS. The modification of NC coatings using sorbitol or citric acid, respectively, led to durable coatings and improved barrier properties. These results show the potential of NC as ecological bio-based coating on porous paperboard.

Acknowledgments We would like to thank Bio4Energy (Sweden) for financially supporting this research.

References

Aulin C, Gällstedt M, Lindström T (2010) Oxygen and oil barrier properties of microfibrillated cellulose films and coatings. Cellulose 17:559–574

Belbekhouche S, Bras J, Siqueira G, Chappey C, Lebrun L (2011) Water sorption behavior and gas barrier properties of cellulose whiskers and microfibrils films. Carbohydr Polym 83:1740–1748

Chinga-Carrasco G, Syverud K (2012) On the structure and oxygen transmission rate of biodegradable cellulose nanobarriers. Nanoscale Res Lett 7:192

De Cuadro P, Belt T, Kontturi K, Kontturi E, Vuorinen T, Hughes M (2015) Cross-linking of cellulose and poly(-ethylene glycol) with citric acid. React Func Polym 90:21–24

Hansen N, Blomfeldt T, Hedenqvist M, Plackett D (2012) Properties of plasticized composite films prepared from naofibrillated cellulose and birch wood xylan. Cellulose 19:2015–2031

Herrera MA, Mathew AP, Oksman K (2014) Gas permeability and selectivity of cellulose nanocrystals films (layers) deposited by spin coating. Carbohydr Polym 112:494–501

Herrera MA, Sirviö JA, Mathew AP, Oksman K (2016) Environmental friendly and sustainable gas barrier on porous materials: nanocellulose coatings prepared using spin- and dip-coating. Mater Des 93:19–25

Joly C, Le Cerf D, Chappey C, Langevin D, Muller G (1999) Residual solvent effect on the permeation properties of fluorinated polyimide films. Separ Purif Technol 16:47–54

Lange J, Wyser Y (2003) Recent innovations in barrier technologies for plastic packaging–a review. Packag Technol Sci 16:149–158

Lavoine N, Bras J, Desloges I (2014) Mechanical ad barrier properties of cardboard and 3D packaging coated with microfibrillated cellulose. J Appl Polym Sci 131:40106

Li F, Biagioni P, Bollani M, Maccagnan A, Piergiovanni L (2013) Multi functional coating of cellulose nanocrystals for flexible packaging applications. Cellulose 20:2491–2504

Liu X, Pang J, Zhang X, Wu Y, Sun R (2013) Regenerated cellulose film with enhanced tensile strength prepared with ionic liquid 1-ethyl-3-methylimidazolium acetate (EMIMAc). Cellulose 20:1391–1399

Mathew AP, Dufresne A (2002) Morphological investigation of nanocomposites from sorbitol plasticized starch and tunicin whiskers. Biomacromol 3:609–617

Mathew A, Thielemans W, Dufresne A (2008) Mechanical properties of nanocomposites from sorbitol plasticized starch and tunicin whiskers. J Appl Polym Sci 109:4065–4074

Mathew AP, Oksman K, Karim Z, Liu P, Khan S, Naseri N (2014) Process scale up and characterization of wood cellulose nanocrystals hydrolyzed using bioethanol pilot plant. Ind Crops Prod 58:212–219

Matsumura H, Sugiyama J, Wolfgang G (2000) Cellulosic nanocomposites. I. Thermally deformable cellulosic hexanoates from heterogeneous reaction. J Appl Polym Sci 78:2242–2253

Moberg T, Sahlin K, Yao K, Geng S, Westman G, Zhou Q, Oksman K, Rigdahl M (2017) Rheological properties of nanocellulose suspensions: effects of fibril/particle dimensions and surface characteristics. Cellulose 24:2499. doi:10.1007/s10570-017-1283-0

Muller-Dethlefs K, Hobza P (2000) Noncovalent interactions: a challenge for experimental theory. Chem Rev 100:143–168

Pasupuleti S, Madras G (2011) Synthesis and degradation of sorbitol-based polymers. J Appl Polym Sci 121:2861–2869

Peroval C, Debeaufort F, Despre D, Voilley A (2002) Edibe arabinoxylan-based films. 1. Effects of lipid type on water vapor permeability, films structure, and other physical characteristics. J Agricult Food Chem 50:3977–3983

Quellmalz A, Mihranyan A (2015) Citric acid cross-linked nanocellulose-based paper for size-exclusion nanofiltration. ACS Biomater Sci Eng 1:271–276

Rodionova G, Hoff B, Lenes M, Eriksen O, Gregersen O (2010) Surface chemical modification of microfibrillated cellulose: improvement of barrier properties for packaging applications. Cellulose 18:127–134

Sirviö J, Kolehmainen A, Liimatainen H, Niinimäki J, Hormi O (2014) Biocomposite cellulose-alginate films: promising packaging materials. Food Chem 151:343–351

Sugiyama J, Vuong R, Chanzy H (1991) Electron diffraction study on the two crystalline phases occurring in native cellulose from an algal cell wall. Macromolecules 24:4168–4175

Syverud K, Stenius P (2009) Strength and barrier properties of MFC films. Cellulose 16:75–85

Thanh N, Nhung H. (2009) Cellulose modified with citric acid and its absorption of PB^{2+} and Cd^{2+} ions. In: Proceedings of the 13th International Electronic Conference on Synthetic Organic Chemistry (pp. 1–13)

Tammelin T, Vartiainen, J. (2014) Nanocellulose films and barriers. In: K. Oksman, AP Mathew, A Bismarck, O Rojas, M Sain (Eds.) Handbook of Green Materials. Self- and direct assembling of bionanomaterials. World Scientific Publisher Vol 3. (pp. 213–229)

Vuoti S, Talja R, Johansson L, Heikkinen H, Tammelin T (2013) Solvent impact on esterification and film formation ability of nanofibrillated cellulose. Cellulose 20:2359–2370

Wang S, Peng X, Zhong L, Jing S, Cao X (2015) Choline Chloride/urea as an effective plasticizer for production of cellulose films. Carbohydr Polym 117:133–139

Xiao C, Zhang Z, Zhang J, Lu Y, Zhang L (2003) Properties of regenerated cellulose films plasticized with α-monoglycerides. J Appl Polym Sci 89:3500–3505

Yoo B, Lee CM (1993) Thermoprotective effect of sorbitol on proteins during dehydration. J Agricult Food Chem 41:190–192

Zhou YJ, Luner P, Caluwe P (1995) Mechanism of cross-linking of paper with polyfunctional carboxylic acids. J Appl Polym Sci 58:1523–1534